

Univerza v Ljubljani
Fakulteta za *matematiko in fiziko*



Energetics of entangled nematic colloids

M. Ravnik, U. Tkalec, S. Copar, S. Zumer, I. Musevic

Faculty of Mathematics and Physics, University of Ljubljana, Ljubljana, Slovenia

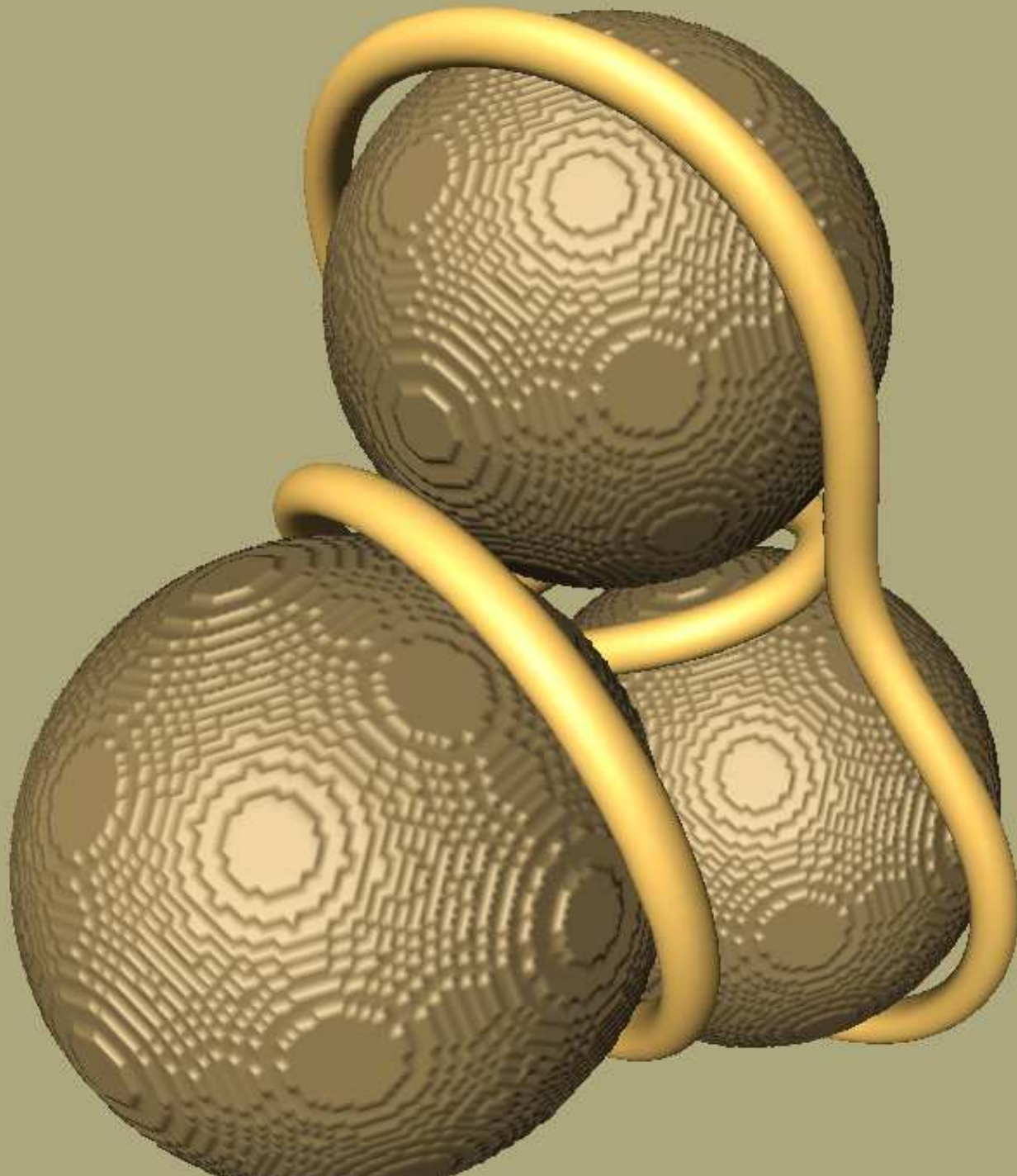
Josef Stefan Institute, Ljubljana, Slovenia

CO NAMASTE

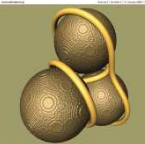
See also talks by Zumer and Musevic

Support of the EC under the Marie Curie project FREEFLUID is acknowledged. The contents reflect only the author's views and not the views of the EC.



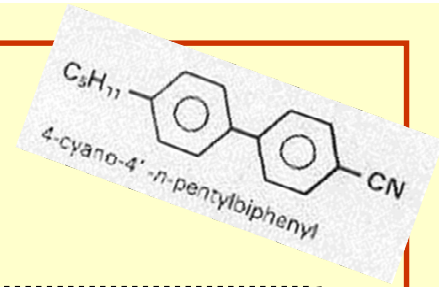


Soft Matter

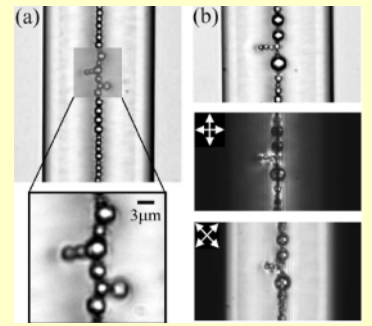
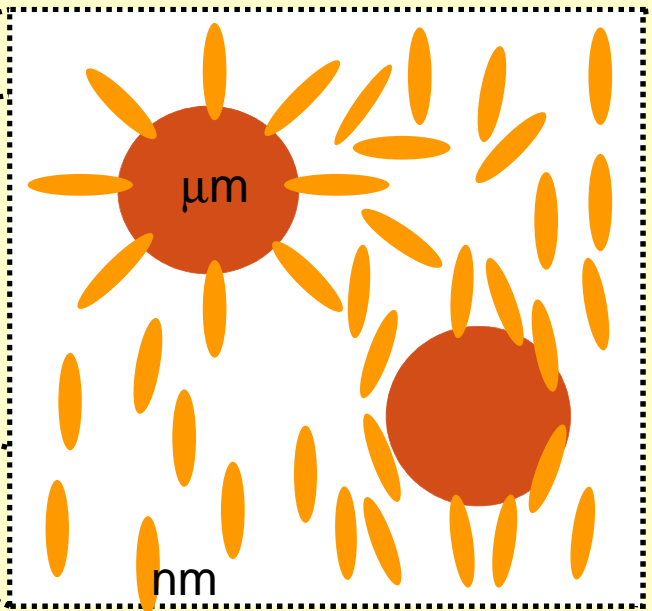
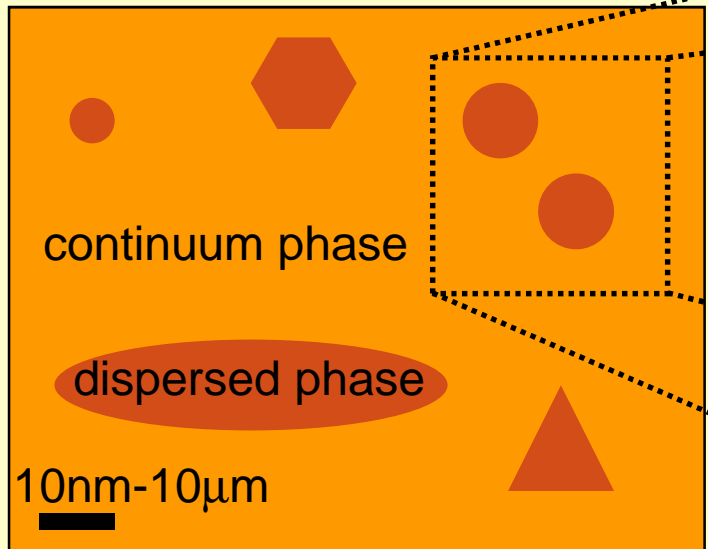


© 2014 Wiley Periodicals, Inc. | www.interscience.wiley.com | ISSN 1522-2775

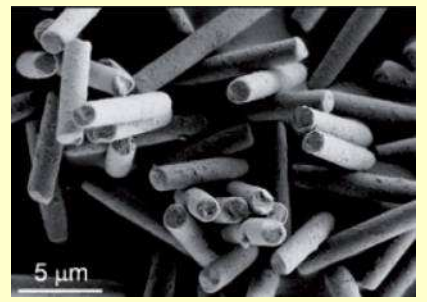
Introduction



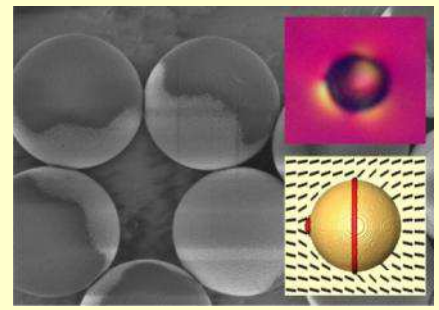
Nematic colloids:



PDMS polymer droplets, Kossyrev et al, PRL 2006



Micro-rods, Tkalec et al, Soft Matter 2008

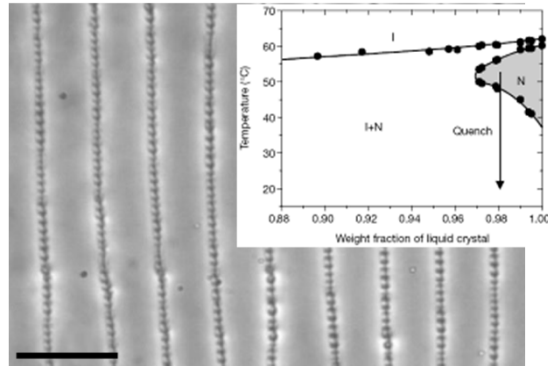


Janus nematic colloids, Conradi et al, Soft Matter 2009

Motivation – optical structures & advanced materials

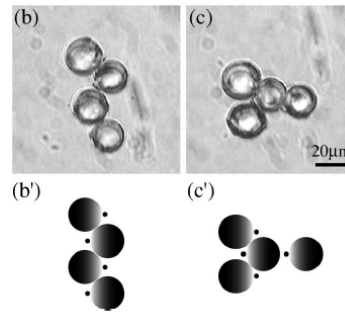
(i) Self assembly of optical structures:

Colloidal chains:



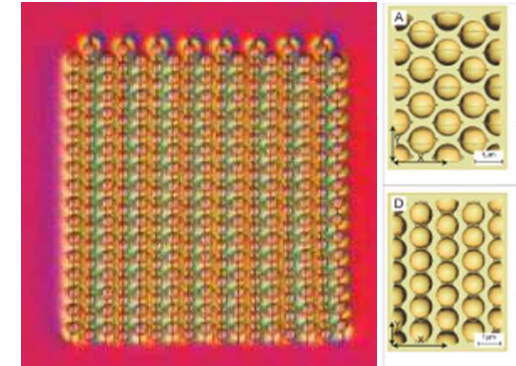
J.-C. Loudet, et al, Nature 407, 611(2000)

Colloidal clusters:



M. Yada, et al, PRL 92, 185501(2004)

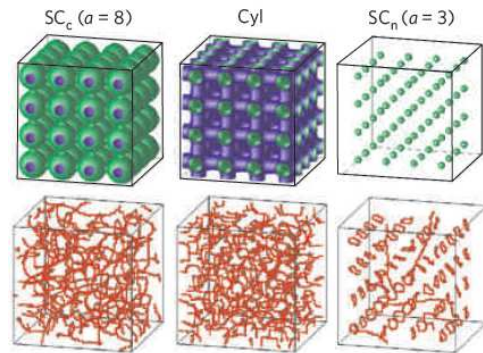
2D colloidal crystals:



I. Musevic, et al, Science 313, 954 (2006)

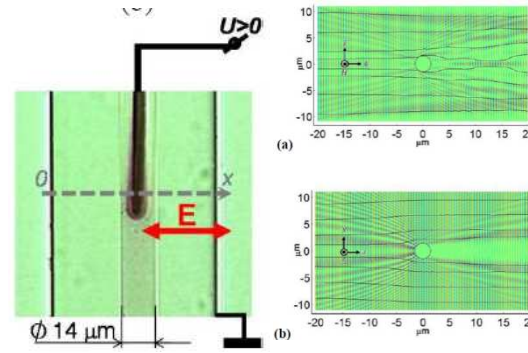
(ii) Advanced material characteristics:

Memory & topological frustration:



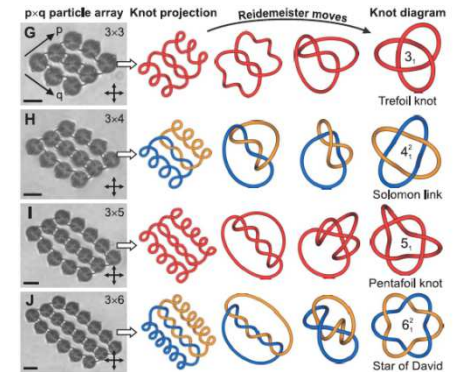
T. Araki, et al, Nat. Mater. 10, 303 (2011)

Tunable transformation optics:



A. B. Golovin, et al, Materials 4, 390 (2011)

Colloidal knots:



U. Tkalec, et al, Science 333, 62 (2011)

Motivation - photonics

Basic interest in liquid crystal colloids is for their application in optics:

Metamaterials and negative refraction (V. G. Veselago, *Sov. Phys. Usp.* **10**, 509 (1968))

D. Smith, et al, *Science* **305**, 788 (2004)

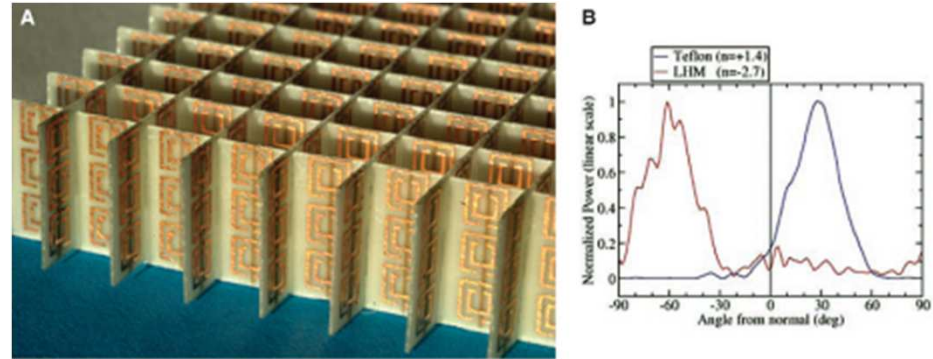
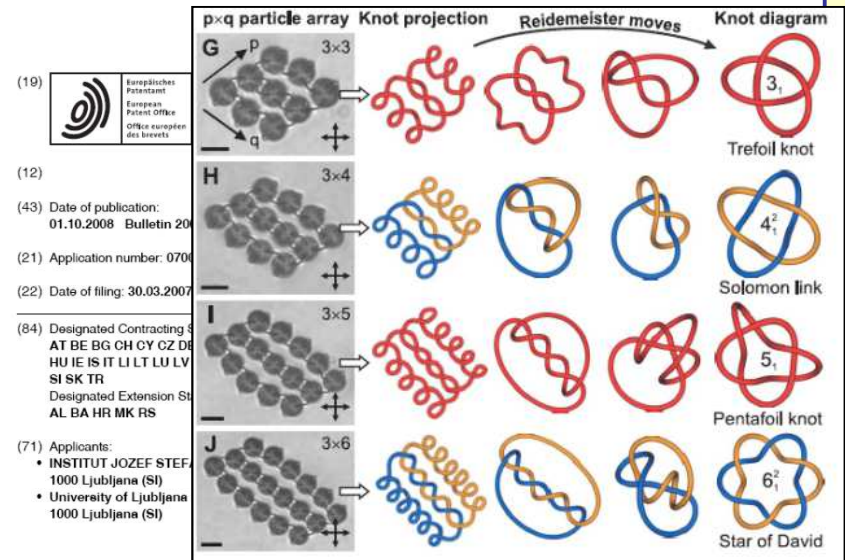
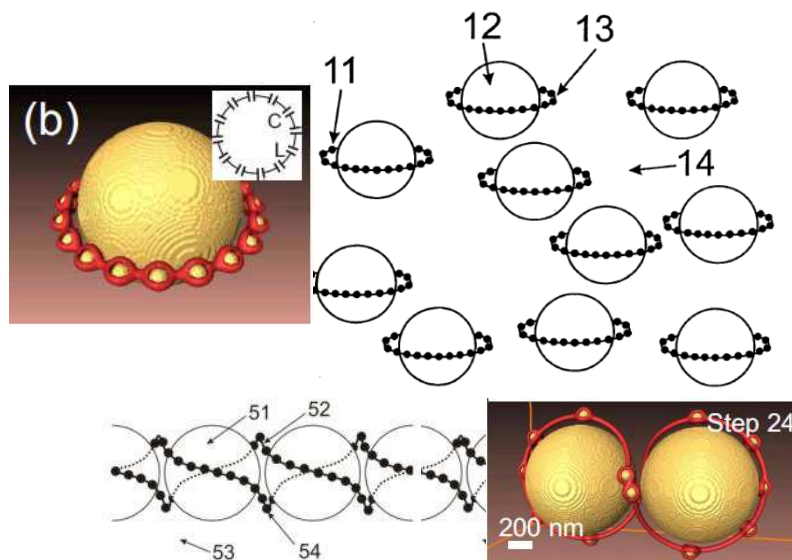


Fig. 3. (A) A negative index metamaterial formed by SRRs and wires deposited on opposite sides lithographically on standard circuit board. The height of the structure is 1 cm. (B) The power detected as a function of angle in a Snell's law experiment performed on a Teflon sample (blue curve) and a negative index sample (red curve).

Hierarchical LC colloids as metamaterials



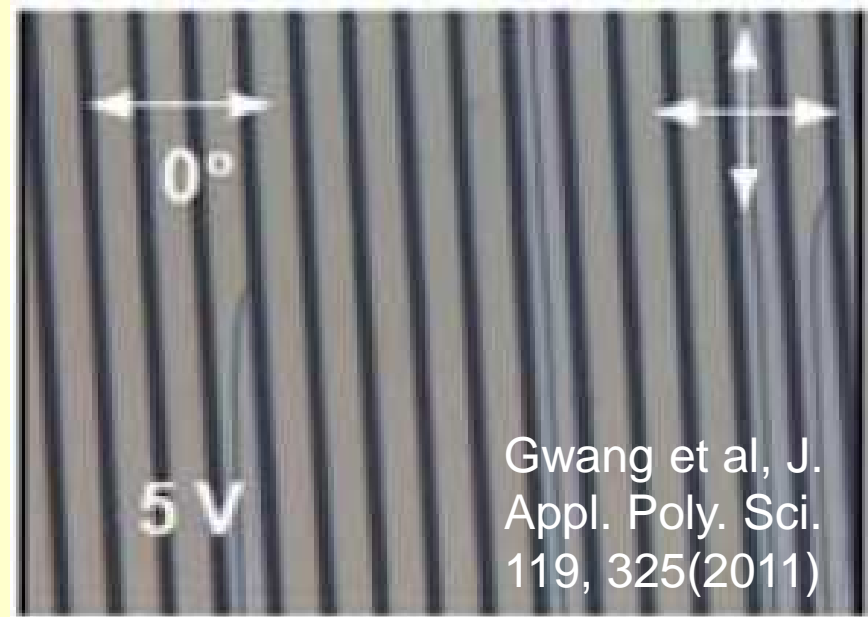
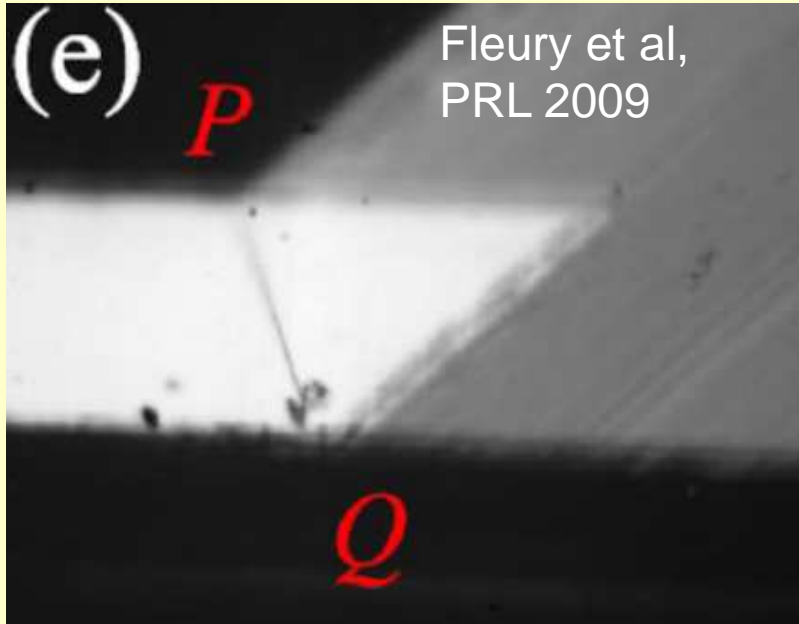
(54) **Metamaterials and resonant materials based on liquid crystal dispersions of colloidal particles and nanoparticles**

Outline

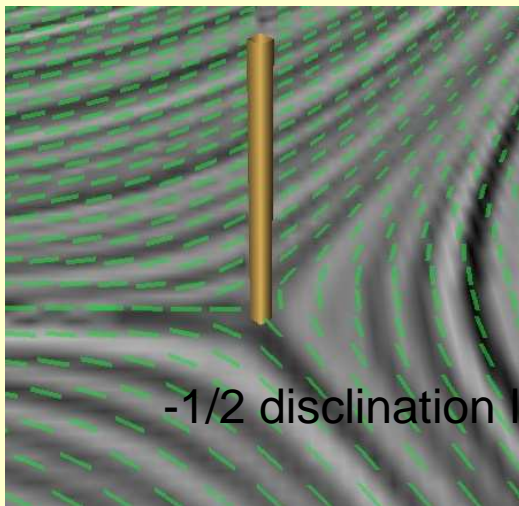


- @ how to generate defect loops in nematics
- @ nematic continuum theory and numerical modelling
- @ entangled nematic colloids and their energetics:
1D, 2D, and 3D structures
- @ energetic stabilisation of topological structures by global twist
- @ assembly of knots and links of defect loops
- @ *blue phases: more complex crossings and caging by defects*
- @ *analogy of chiral liquid crystals and chiral ferromagnets*

Defects in nematic LC

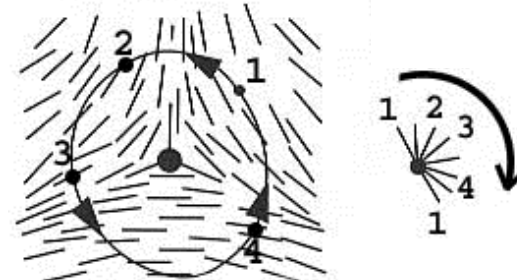


In nematic colloids:



-1/2 disclination line

Winding number

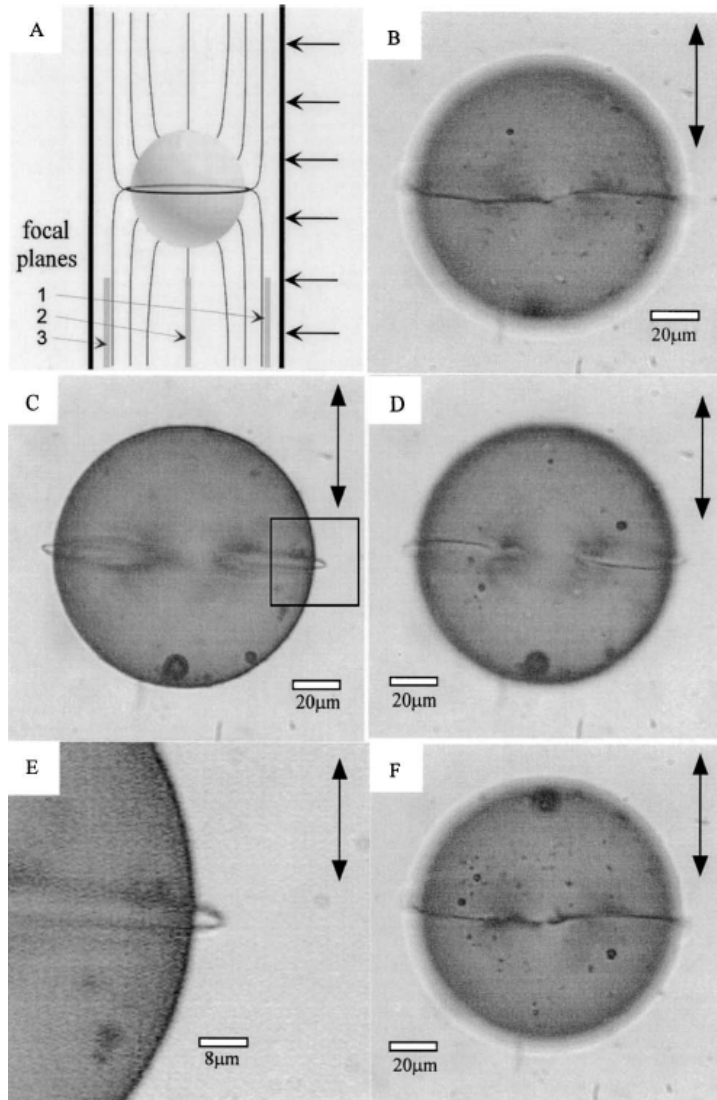


$$\oint d\phi = 2\pi k$$

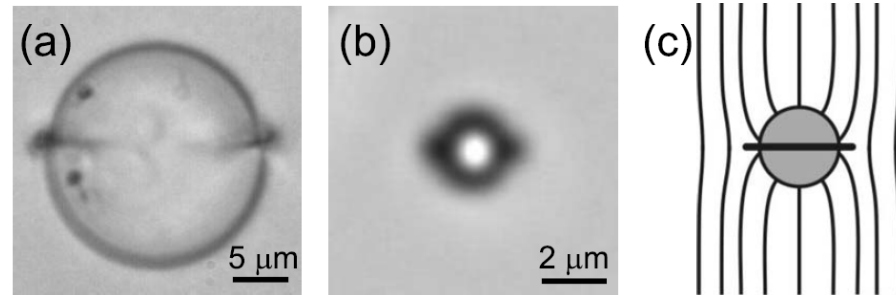
$\rightarrow k = -1/2$

Defect loops in nematic colloids

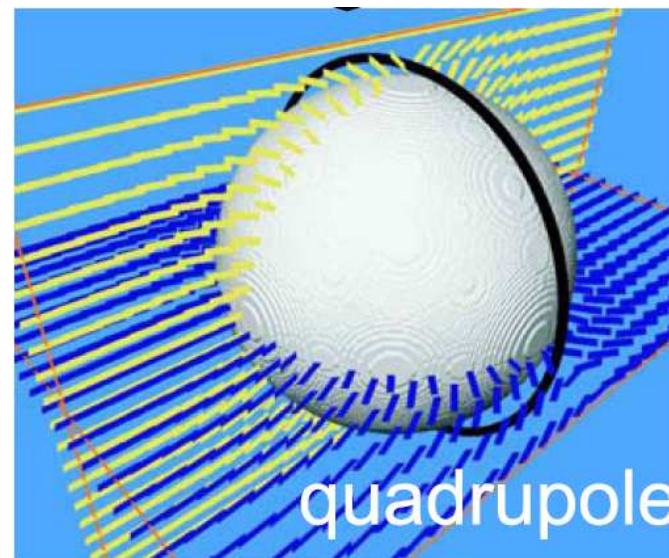
Defect loops form naturally in nematic colloids with HOMEOTROPIC anchoring:



Gu&Abbott, PRL 2000



Musevic & Zumer group, Science 2006, PRE 2007, 2008, PRL 2008



Elastic quadrupole, Saturn ring

Temperature I-N quench

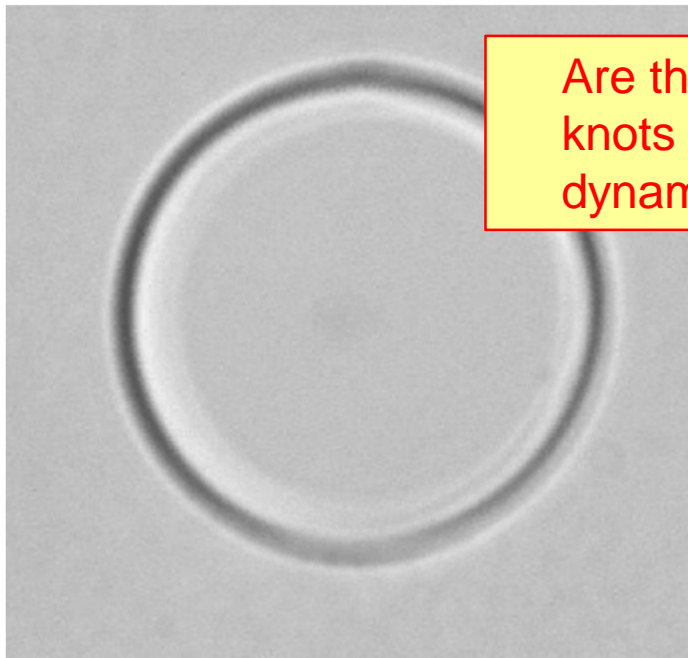
Experimentally:

laser tweezers locally heat the nematic into the isotropic phase;
switch-off the laser beam

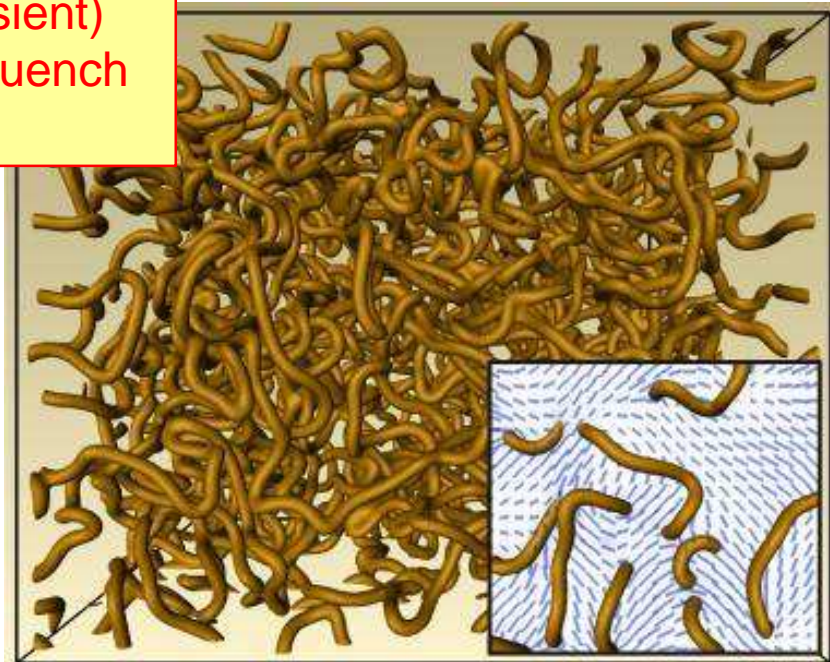
Numerical modelling:

- random initial condition
- relaxation algorithm

$$\Gamma \frac{dQ_{ij}}{dt} = h_{ij}^{\dots}$$



Are there (transient) knots in such quench dynamics?



Courtesy M. Skarabot; real time ~0.1s

Mesoscopic theory of nematic fluids

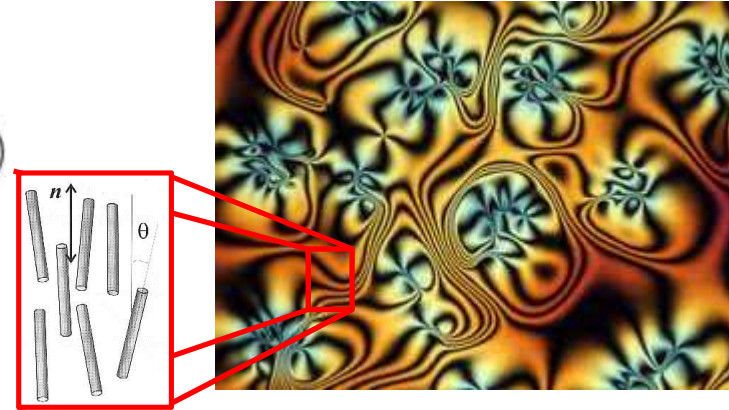
1/3

Order parameter tensor:

$$Q_{ij} = \frac{S}{2}(3n_i n_j - \delta_{ij}) + \frac{P}{2}(e_i^{(1)} e_j^{(1)} - e_i^{(2)} e_j^{(2)})$$

Velocity field and density:

$$u_i, \rho$$



By O. Lavrentovich, LCI, Kent, USA

Q, u and ρ are spatial fields that characterise LC molecules.

I. Equilibrium physics of nematic fluids Landau – de Gennes phenomenological free energy

$$\begin{aligned}
 F = & + \frac{1}{2}L \int_{LC} \left(\frac{\partial Q_{ij}}{\partial x_k} \right) \left(\frac{\partial Q_{ij}}{\partial x_k} \right) dV \quad \leftarrow \text{elasticity} \\
 & + \int_{LC} \left(\frac{1}{2}A Q_{ij} Q_{ji} + \frac{1}{3}B Q_{ij} Q_{jk} Q_{ki} + \frac{1}{4}C (Q_{ij} Q_{ji})^2 \right) dV \quad \leftarrow \text{order} \\
 & + \frac{1}{2}W \int_{Surf.Col.} (Q_{ij} - Q_{ij}^0)(Q_{ji} - Q_{ji}^0) dS \quad \leftarrow \text{surface}
 \end{aligned}$$

Additional coupling terms for external fields, flexoelectricity, chirality...

Mesoscopic theory of nematic fluids

II. Dynamics of liquid crystals

Orientation:

$$(\partial_t + \vec{u} \cdot \nabla) \mathbf{Q} - \mathbf{S}(\mathbf{W}, \mathbf{Q}) = \Gamma \mathbf{H}$$

Material derivative

LC alignment in flow

molecular field

Flow:

Flow aligning: /

Flow tumbling: -

$$\rho(\partial_t + u_\beta \partial_\beta) u_\alpha$$

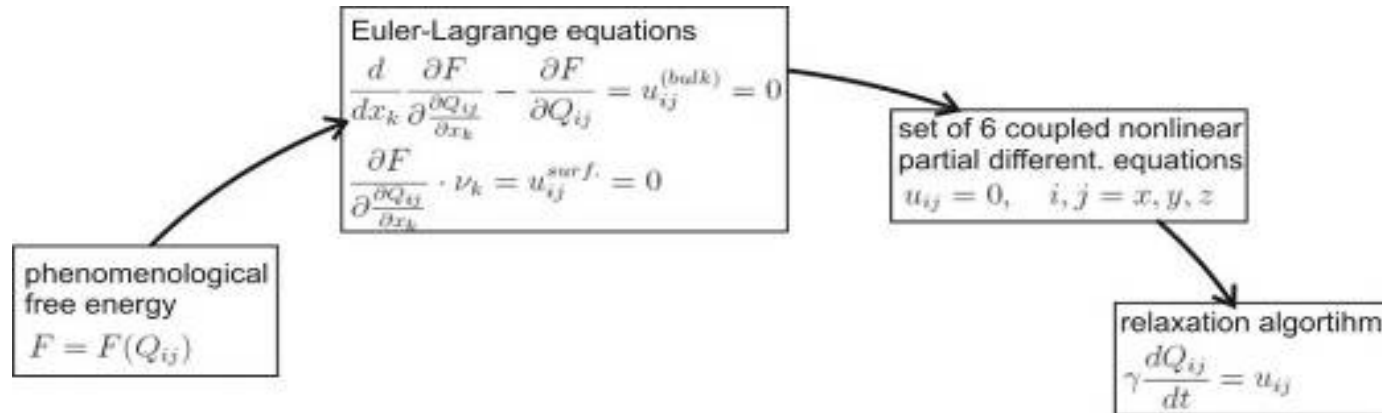
$$= \underbrace{\partial_\beta (\Pi_{\alpha\beta})}_{\text{Stress tensor}} + \underbrace{\eta \partial_\beta (\partial_\alpha u_\beta + \partial_\beta u_\alpha)}_{\text{viscosity}} + \underbrace{(1 - 3\partial_\rho P_0) \partial_\gamma u_\gamma \delta_{\alpha\beta}}_{\text{possible compressibility}}$$

Generalized Navier – Stokes equation

$$\begin{aligned} \Pi_{\alpha\beta} = & -P_0 \delta_{\alpha\beta} + 2\xi \left(Q_{\alpha\beta} + \frac{1}{3} \delta_{\alpha\beta} \right) Q_{\gamma\epsilon} H_{\gamma\epsilon} \\ & - \xi H_{\alpha\gamma} \left(Q_{\gamma\beta} + \frac{1}{3} \delta_{\gamma\beta} \right) - \xi \left(Q_{\alpha\gamma} + \frac{1}{3} \delta_{\alpha\gamma} \right) H_{\gamma\beta} \\ & - \partial_\alpha Q_{\gamma\nu} \frac{\delta \mathcal{F}}{\delta \partial_\beta Q_{\gamma\nu}} + Q_{\alpha\gamma} H_{\gamma\beta} - H_{\alpha\gamma} Q_{\gamma\beta}. \end{aligned}$$

Numerical modelling

A) Equilibrium - Finite difference explicit relaxation algorithm



B) Dynamics - Hybrid Lattice Boltzmann algorithm (developed with J.M. Yeomans, Oxford):

I. Finite differences for Q dynamics:

$$Q_{ij}^{t+\Delta t} = Q_{ij}^t + \frac{\Delta t}{\Gamma} h_{ij}^{\dots, t}$$

II. Lattice Boltzmann method for material flow u and density ρ :

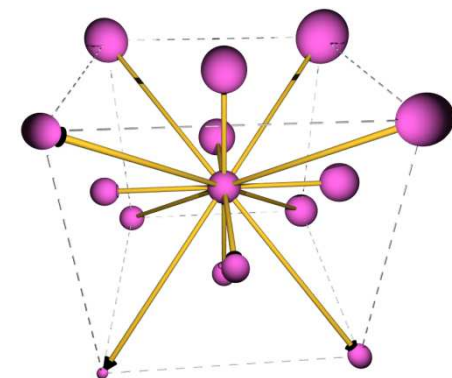
Distribution functions f_i :

$$\rho = \sum_i f_i, \quad \rho u_\alpha = \sum_i f_i e_{i\alpha},$$

Streaming and collision

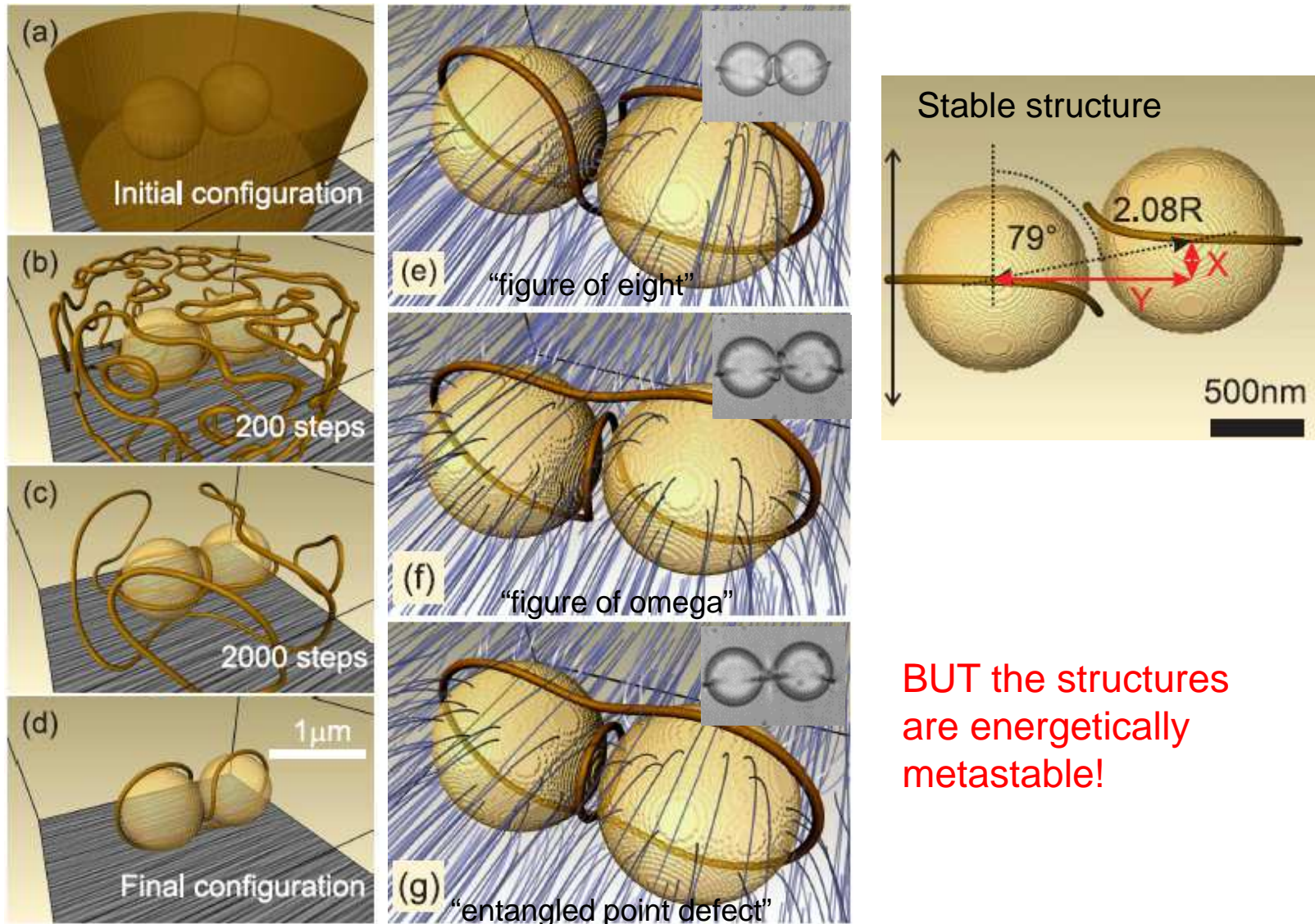
$$f_i(\mathbf{x} + \mathbf{e}_i \Delta t, t + \Delta t) - f_i(\mathbf{x}, t) = -\frac{1}{\tau_f} (f_i(\mathbf{x}, t) - f_i^{\text{eq}}(\mathbf{x}, t, \{f_i\})) + p_i(\mathbf{x}, t, \{f_i\})$$

D3Q15 scheme



1D Entangled structures – complex conformations of defect loops

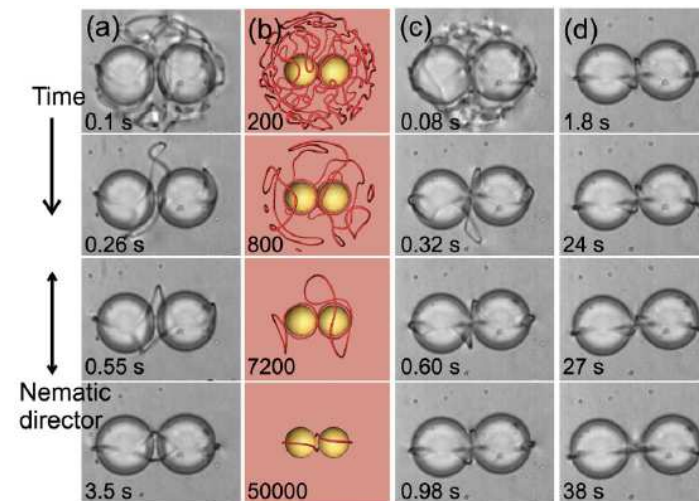
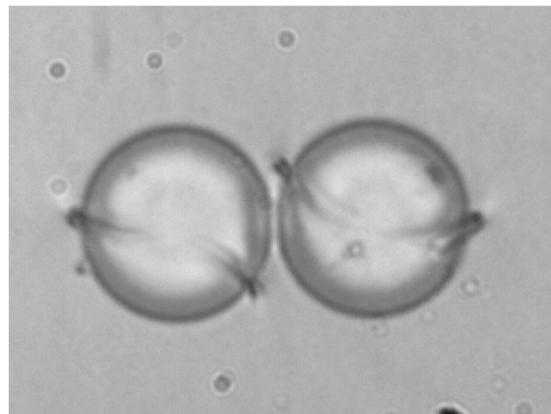
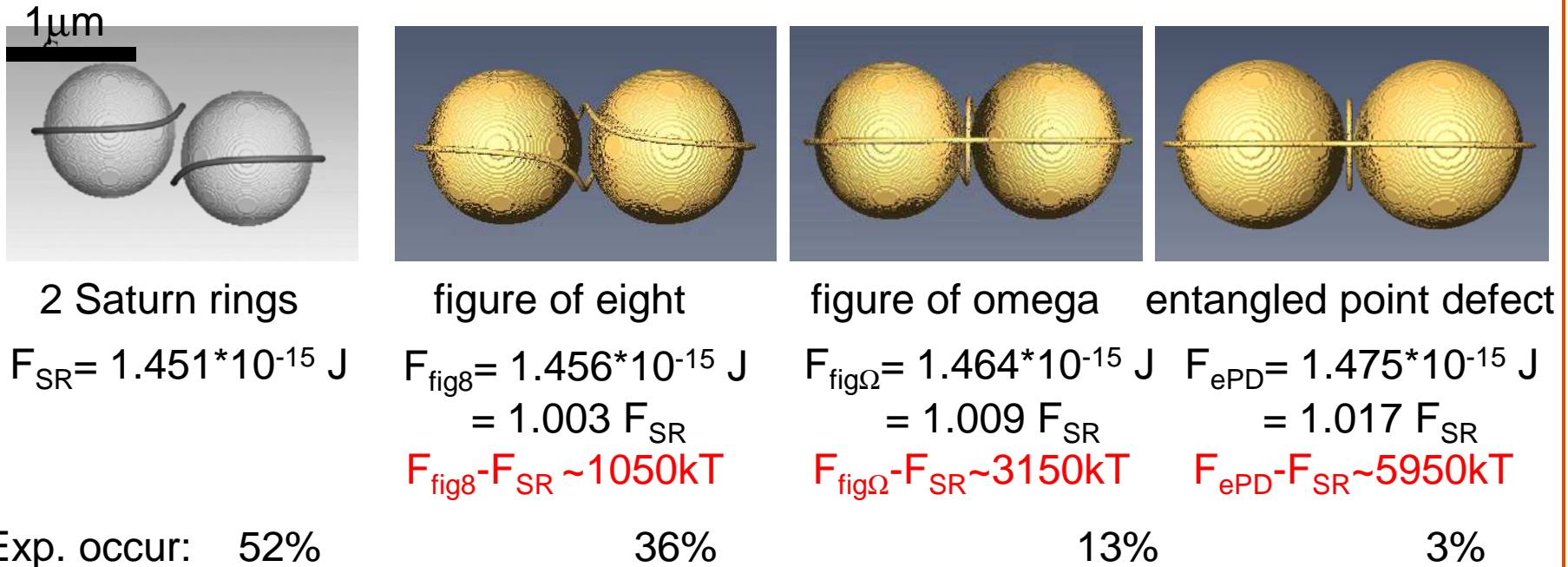
Local I – N temperature quench – now in the region of colloidal particles:



BUT the structures are energetically metastable!

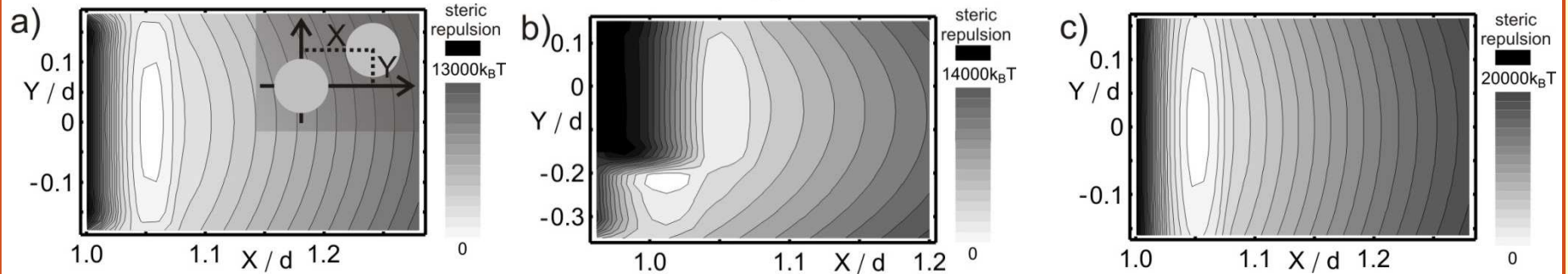
1D Entangled structures –free energies and energy barriers

I. Equilibrium free energies:



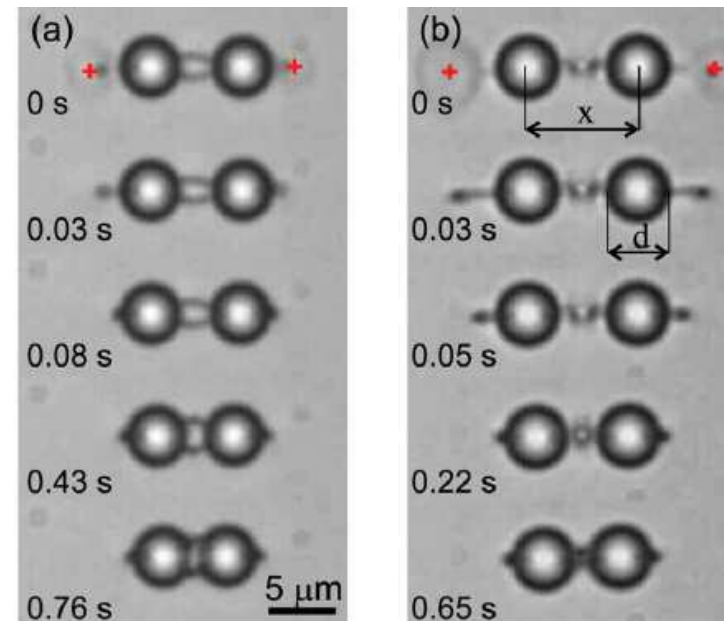
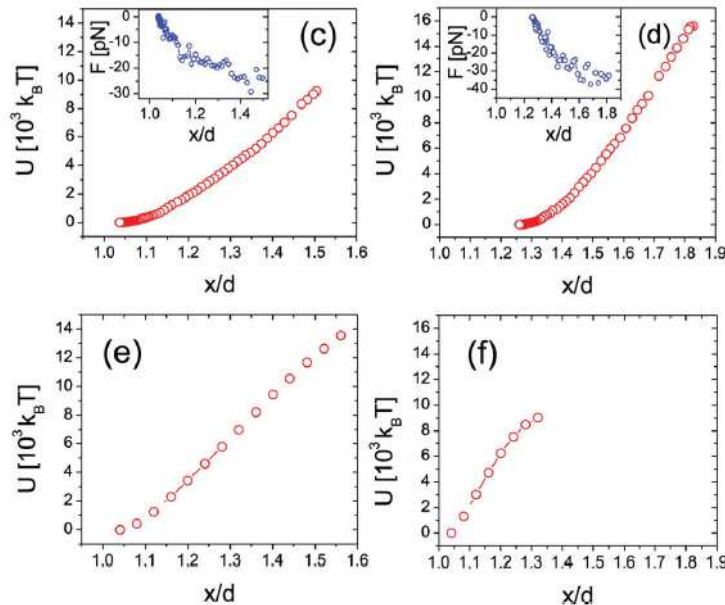
1D Entangled structures – free energies and energy barriers

II. Energy barriers between the states:



Strongly anisotropic energy barriers; minimum heights of $>1000 k_B T$

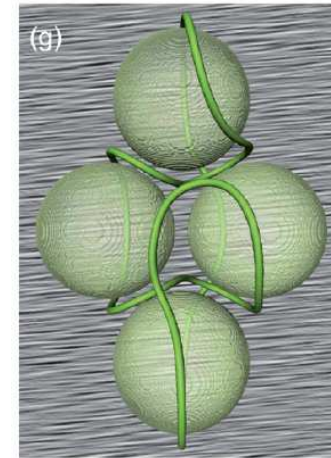
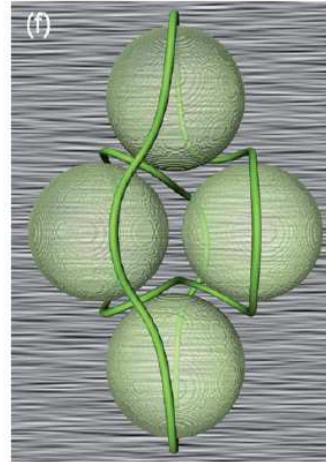
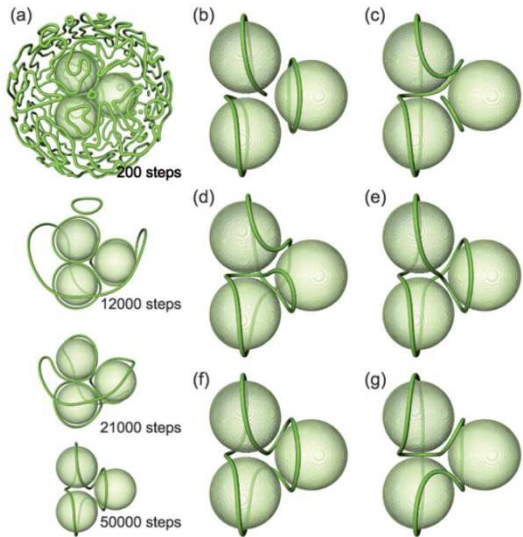
Comparison with experiments:



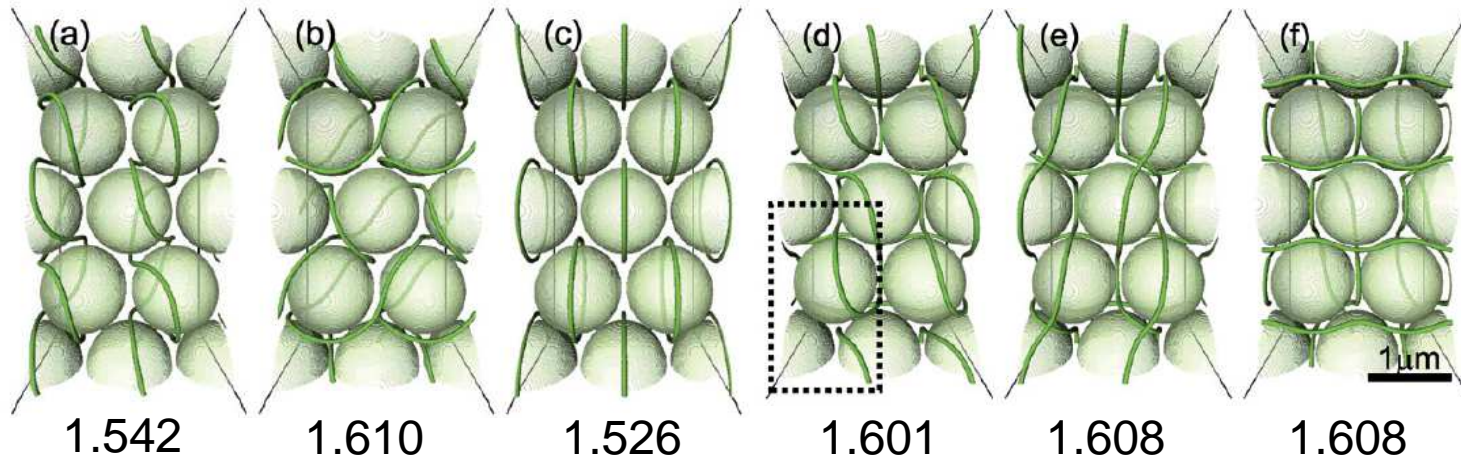
2D entangled structures – conformations of defects in 2D

uniform nematic

Clusters:



2D Colloidal crystals:



Free energies
[fJ/UC]:

1.542

1.610

1.526

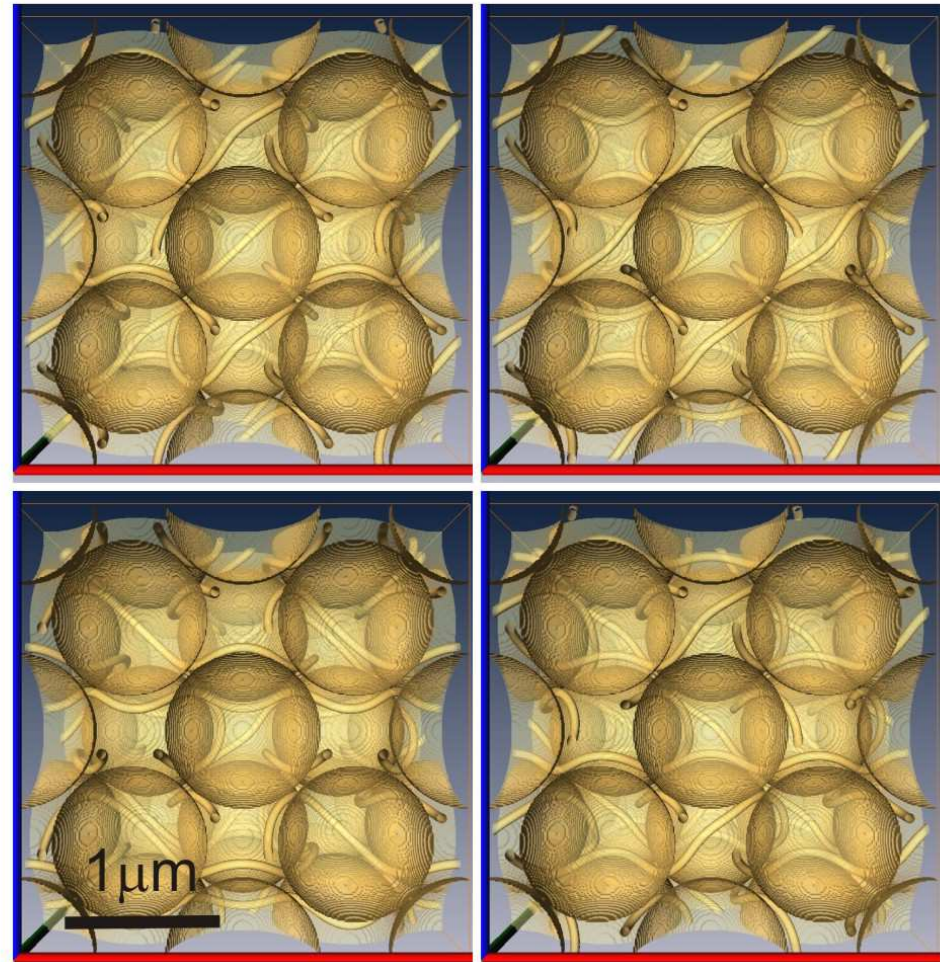
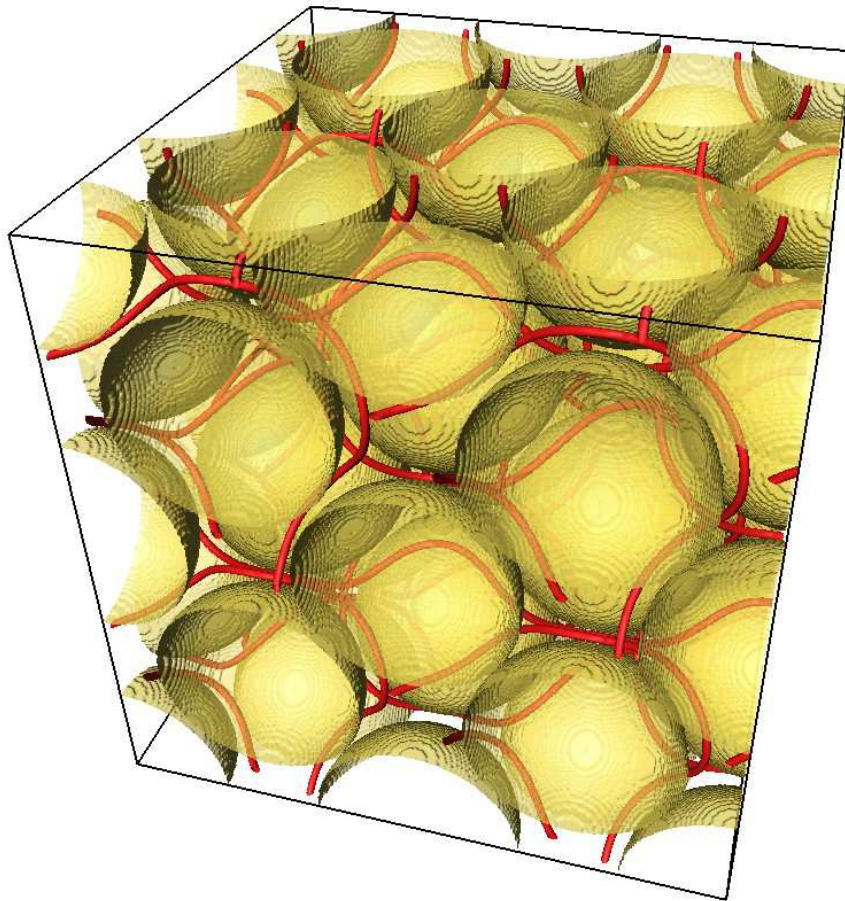
1.601

1.608

1.608

3D entangled colloids - defect motifs spanning in 3D uniform nematic

FCC nematic colloidal opals:

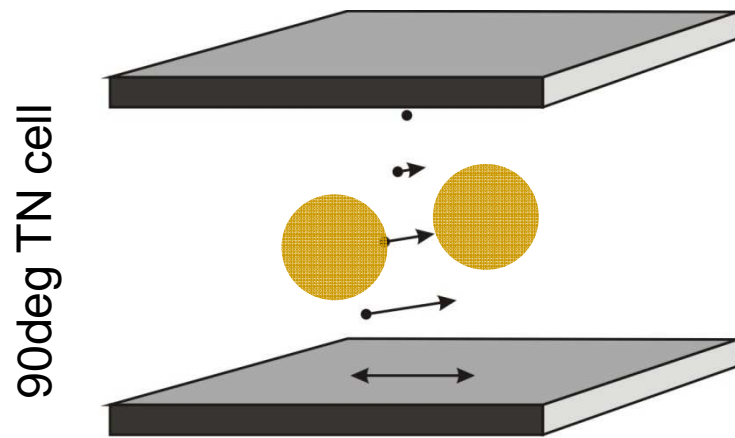


Also, in 3D structures (tetrahedral) rewiring sites emerge, their number depending on the colloidal lattice

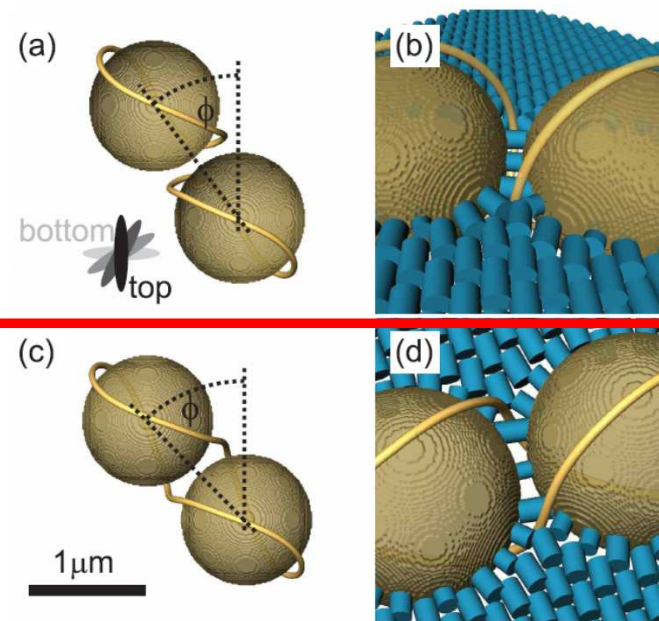
1D Entangled structures – reversing the (meta)stability by twist

Changing the far-field condition reverses stability and metastability of the entangled and non-entangled structures.

Geometry:



Entangled configuration is energetically the most favourable:



Free. En. (Saturn rings) = $1.975 \cdot 10^{-15}$ J

Free. En. (Figure-of-eight) = $1.926 \cdot 10^{-15}$ J

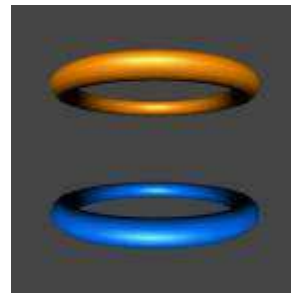
Stable structure with minimum free energy

1D Entangled structures – Hopf link

Defect loops can have various conformations:



2 Saturn ring defects



Unlink

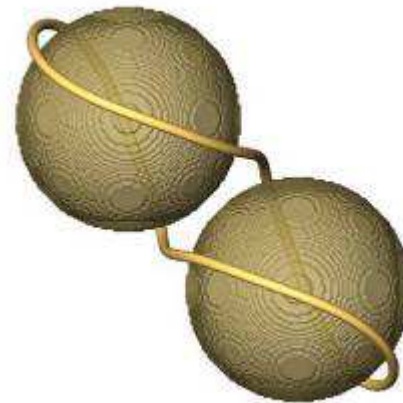
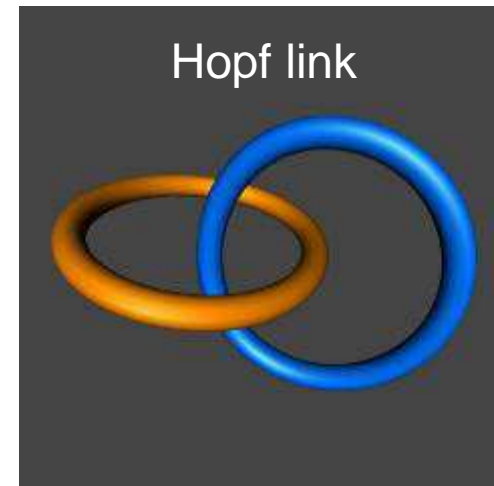
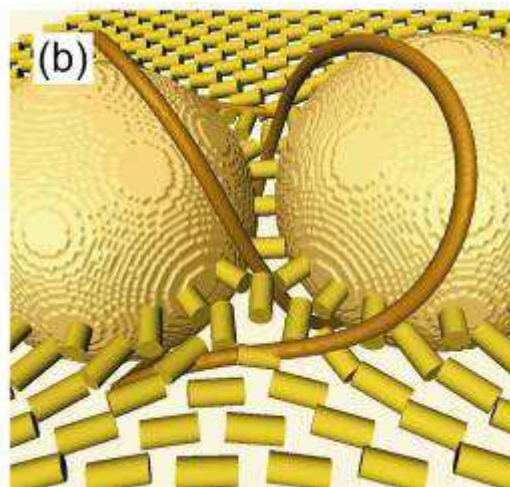
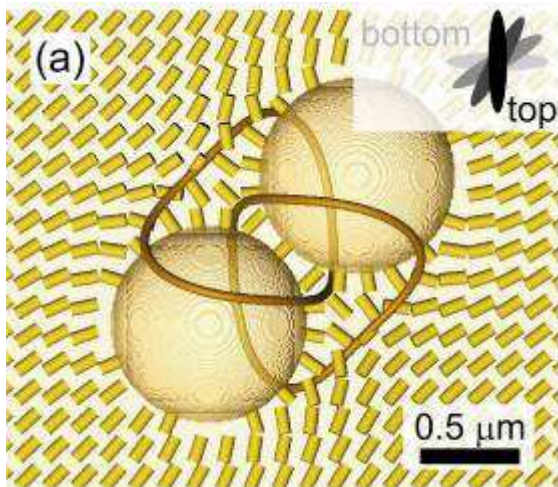


Figure of eight



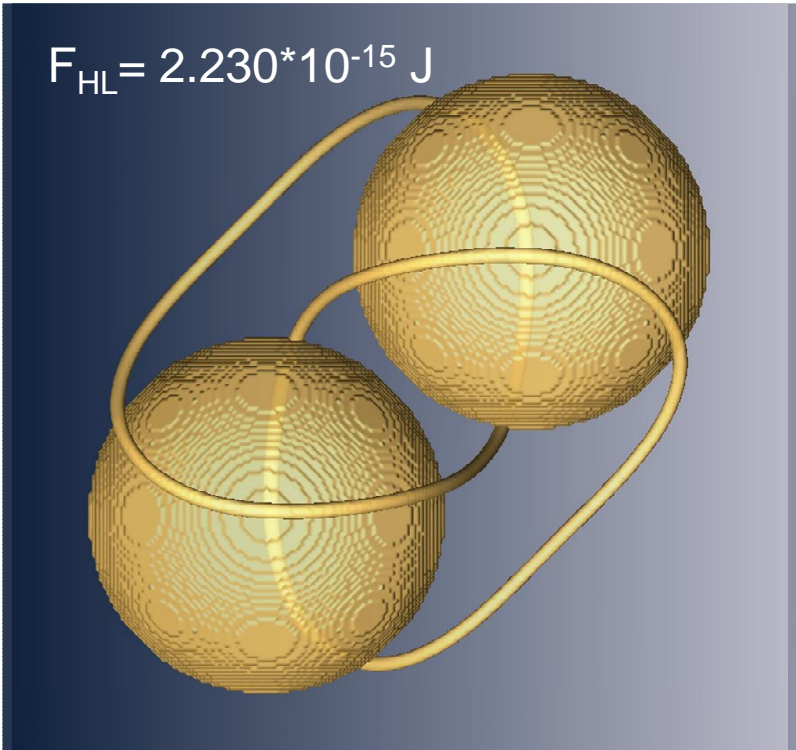
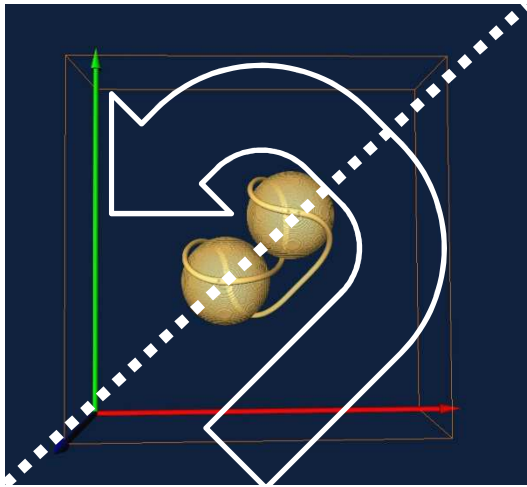
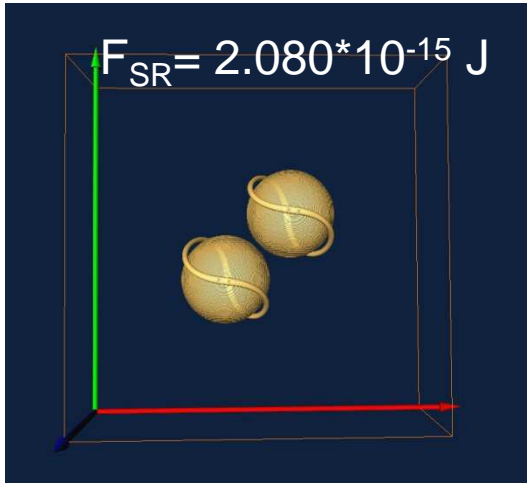
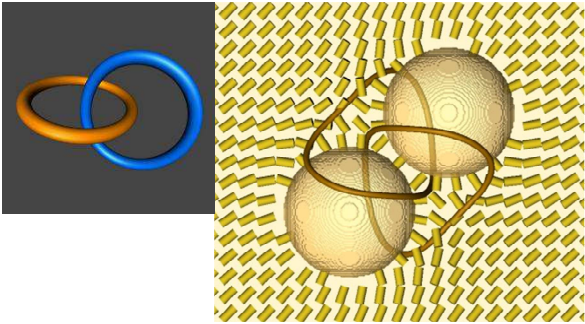
Unknot



Hopf link

1D Entangled structures – Hopf link 2

How to access metastable knotted configurations:



Spontaneously formed colloidal structures– defect braids

Experiments: $\sim 4.7\mu\text{m}$ homeotropic silica particles in $\sim 6\mu\text{m}$ thick 90° TN cell.

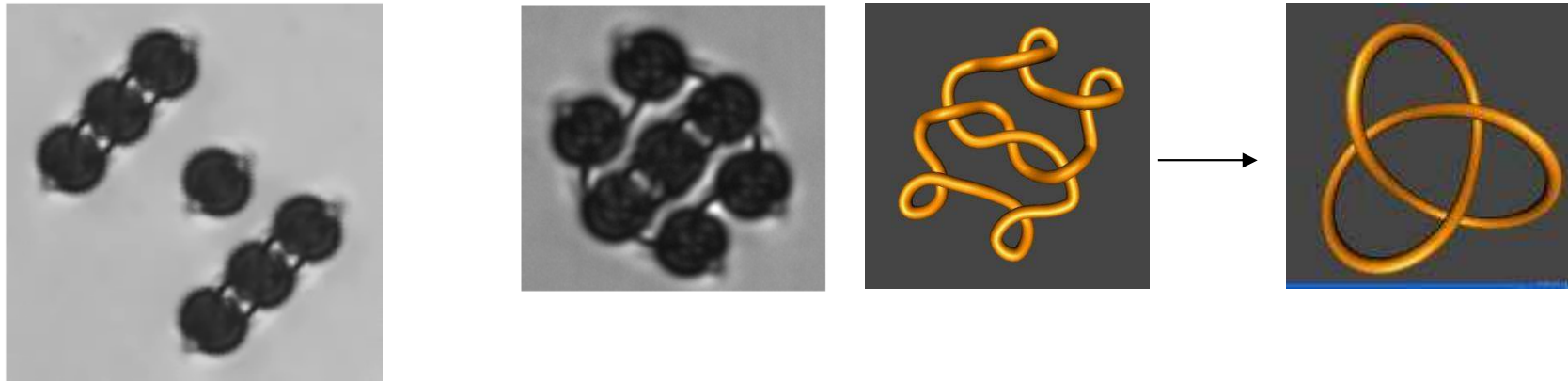


Structures
assembled within
capillary filling of
the nematic cell

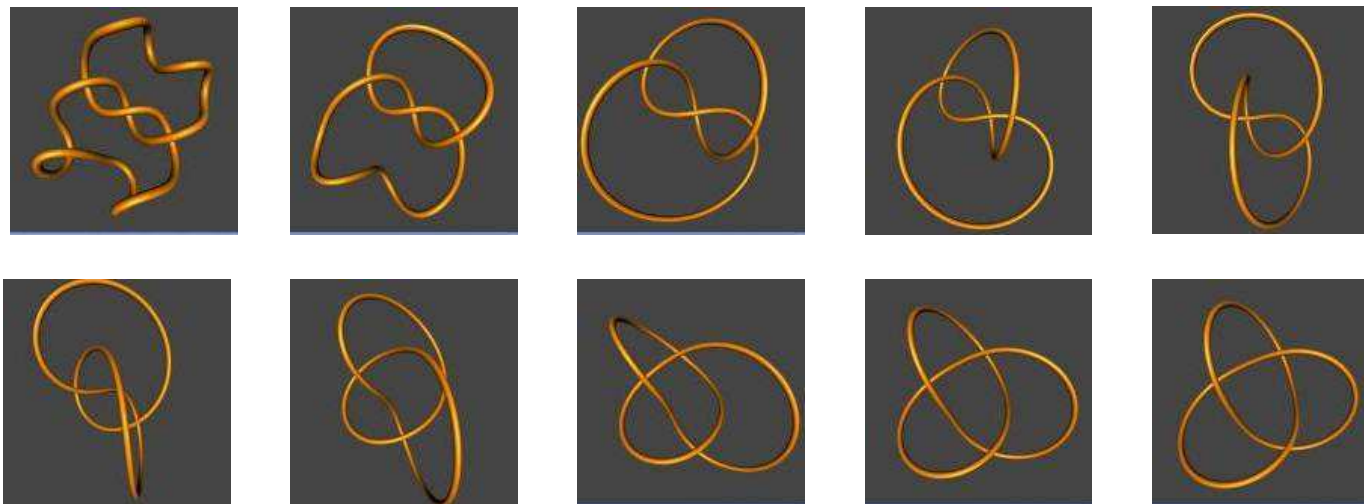
Image courtesy of U. Tkalec

Knots and links – trefoil

Complex initial conformation of the disclination loop is equivalent (isotopic) to the trefoil knot:

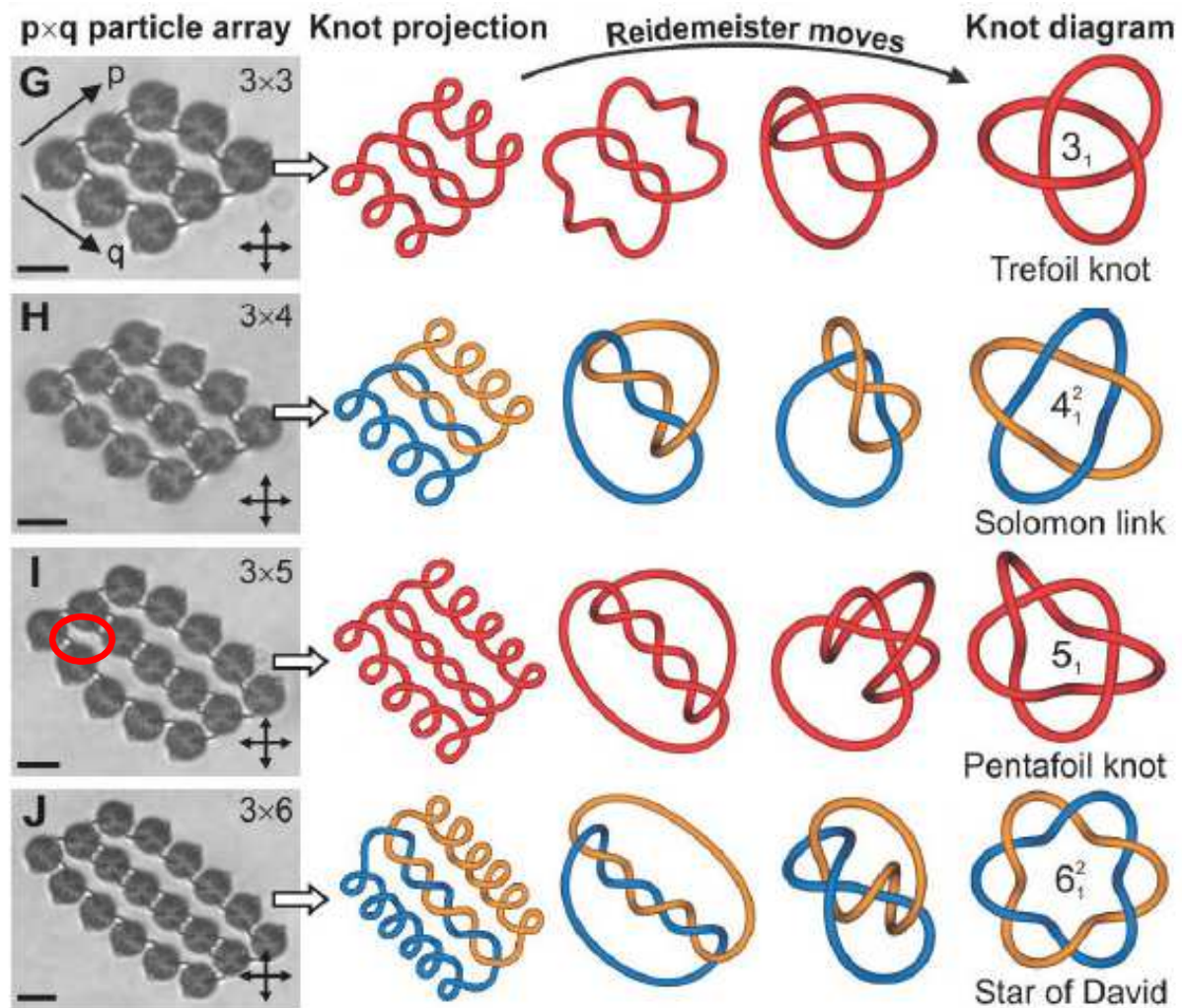


Continuous transformation of the disclination loop (Reidemeister moves):



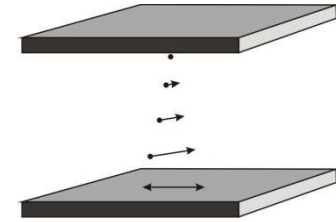
Torus knots and links

Full series of torus knots and links can be assembled

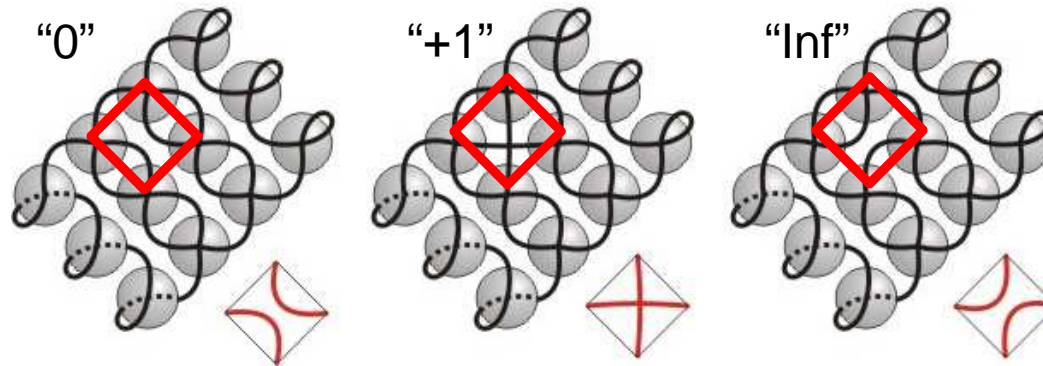


Classification after: V. V. Prasolov, A. B. Sossinsky: Knots, links, braids and 3-manifolds : an introduction to the new invariants in low-dimensional topology (1997)

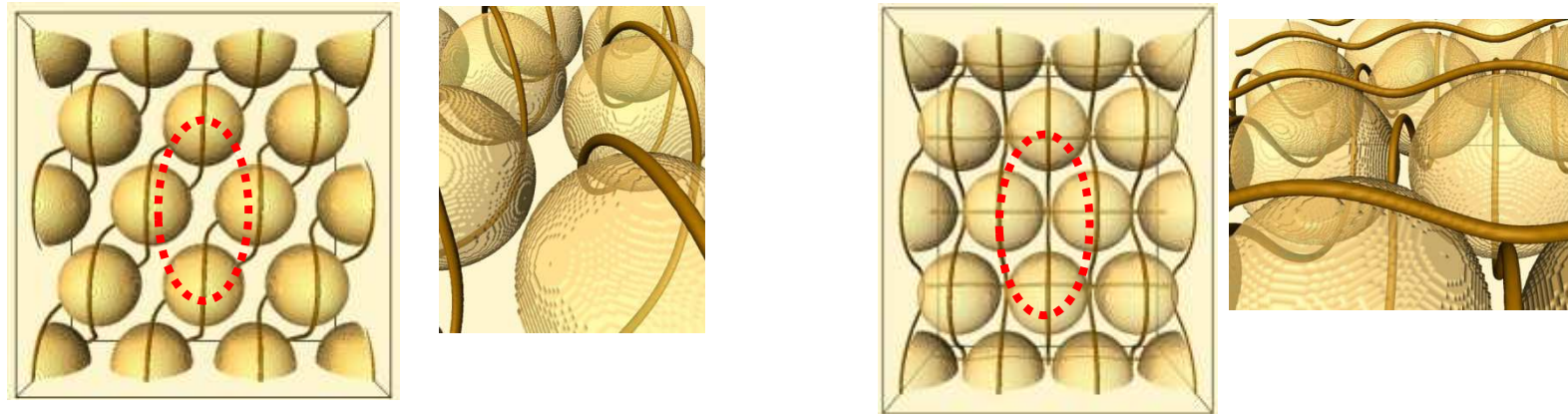
2D entangled structures – structures of tangles



Nematic profile in tangles:



Numerically modelled tangles:



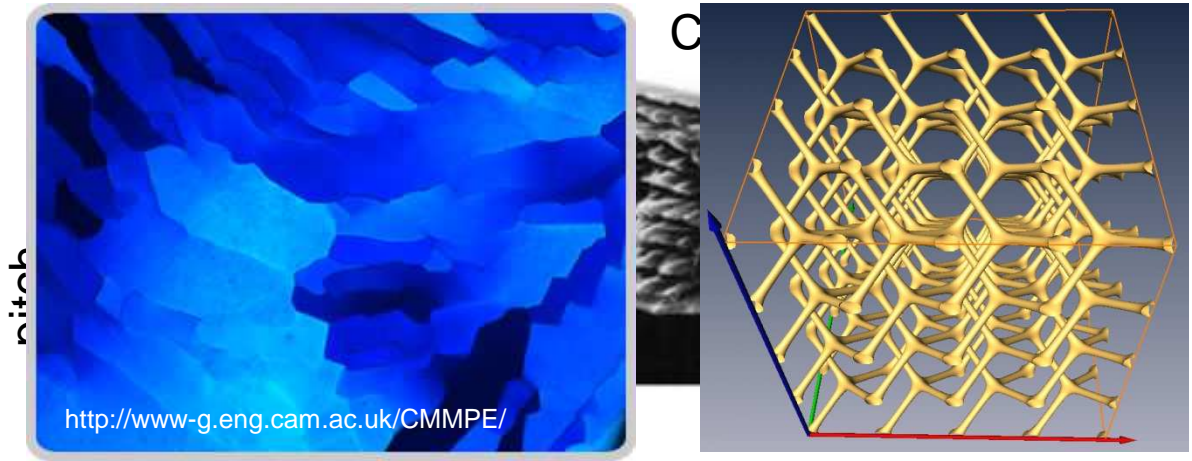
0 and Inf tangle

+1 tangle

Numerically “assembling” the tangle regions gives full knotted nematic fields.

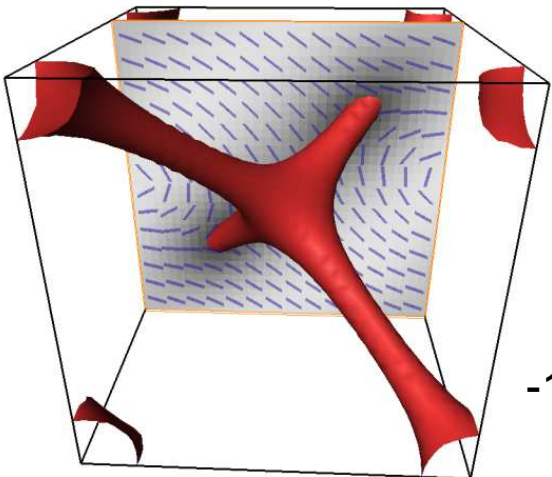
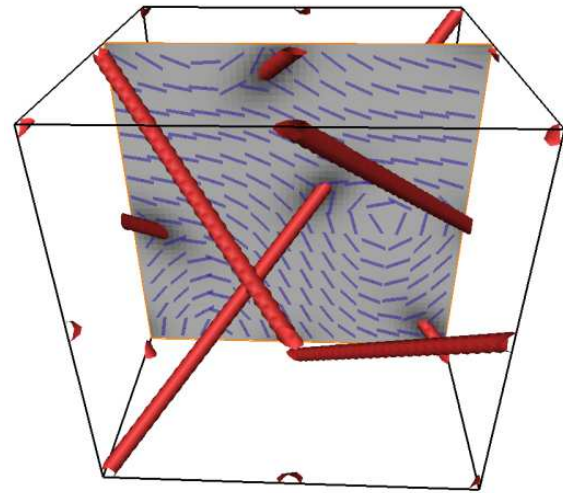
Liquid crystal blue phases – beyond simple crossings 1/3

Liquid crystals with chiral molecules twist spontaneously:



Unit cell of BP I

Unit cell of BP II

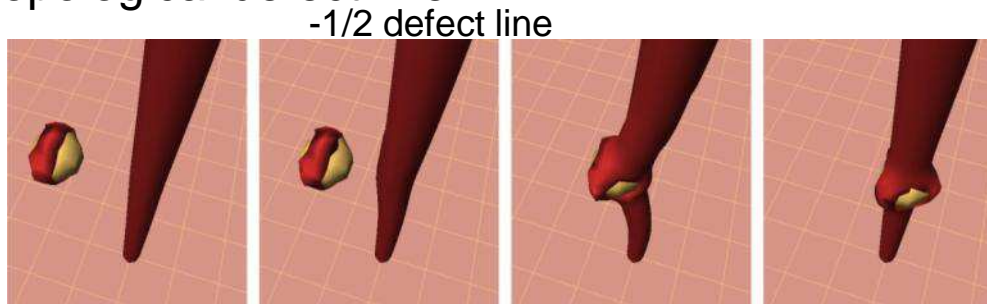


Blue phases are natural progenitors of topological defect lines

-1/2 disclination lines

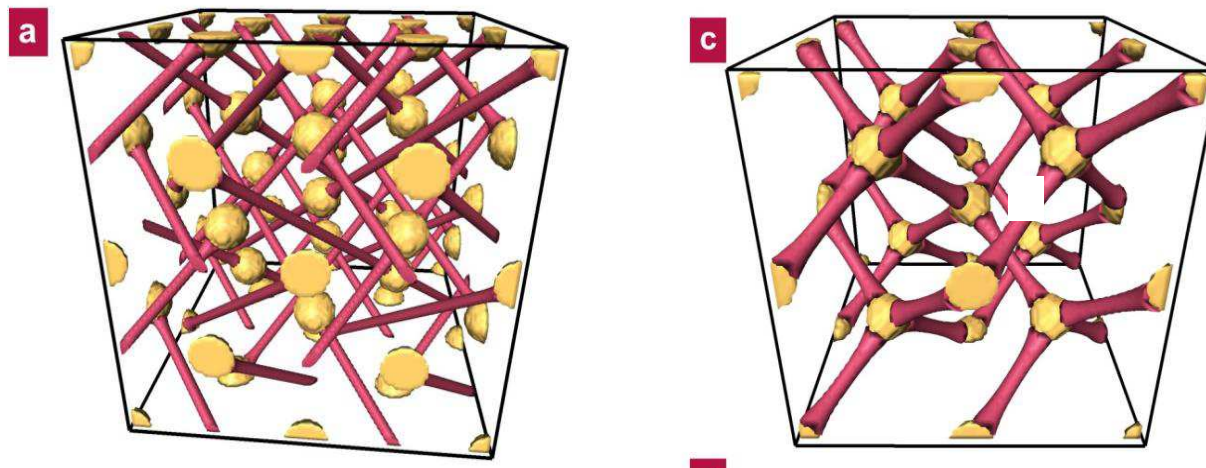
Liquid crystal blue phases – beyond simple crossings 2/3

EFFECTIVE “SPLITTING”: Colloidal particles CAN split the singular core of the topological defect line.



Homeotropic 40nm particle

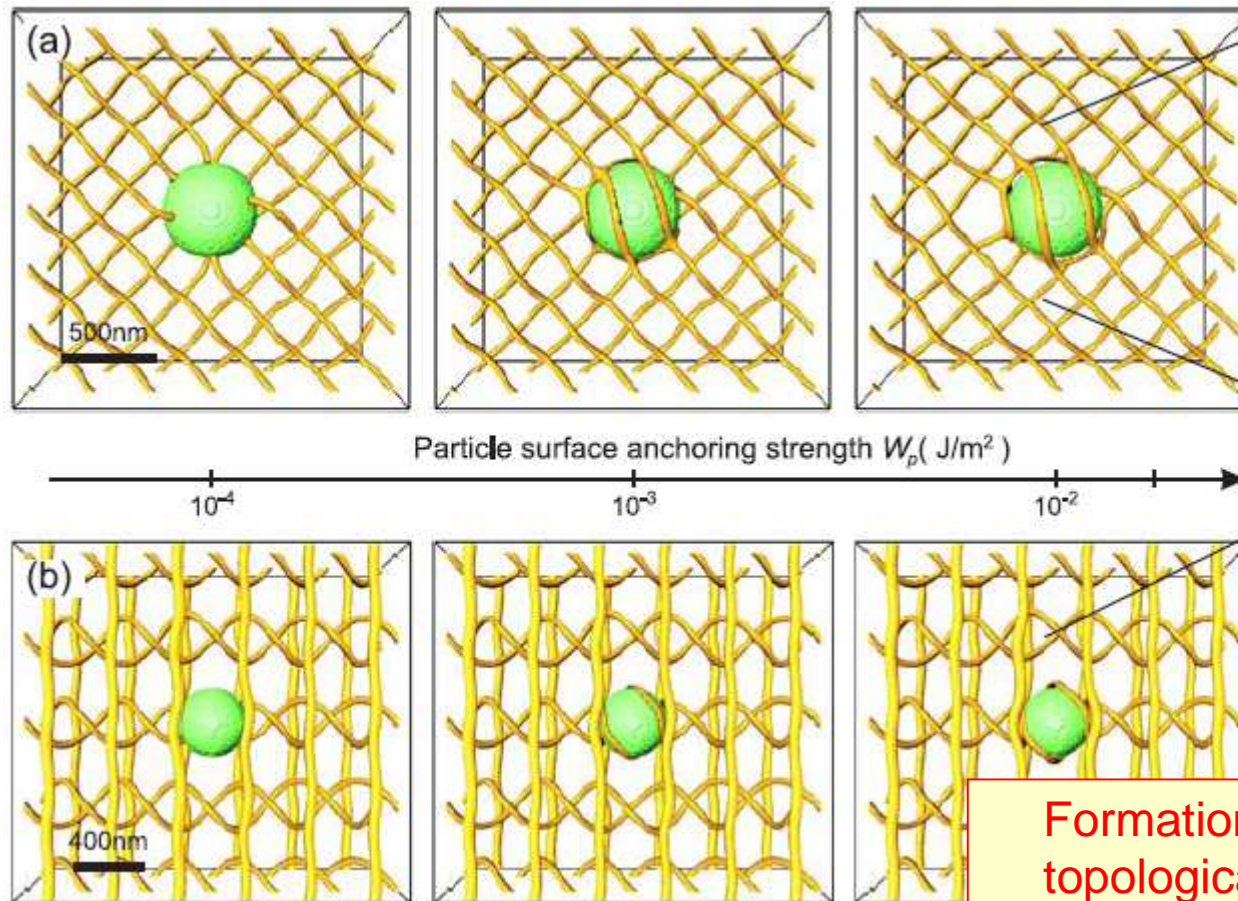
EFFECTIVE CUTTING: Colloidal particles can effectively cut the core of the topological defect line.



Splitting and cutting regime can be tuned by surface interactions

Liquid crystal blue phases – beyond simple crossings 3/3

Confinement of larger particles produces cages of topological defects:

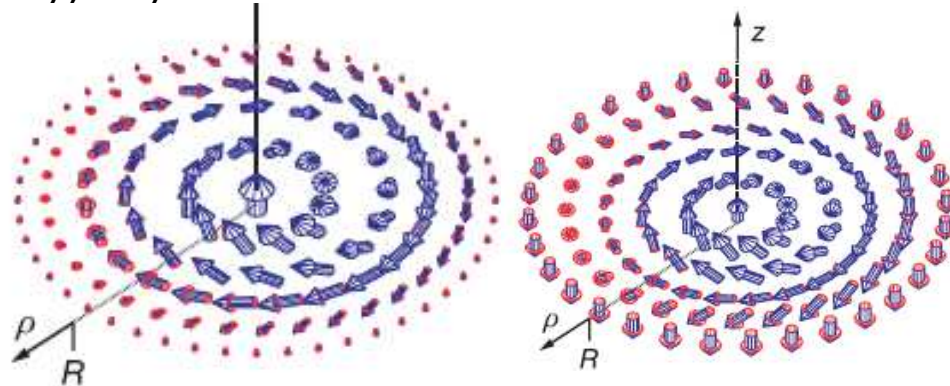


Formation
topologica
“cages”

Interesting topology and rheology.

Analogy: liquid crystals and chiral ferromagnets

Complex topological structures in the magnetisation field of chiral ferromagnets – the (baby) skyrmions:

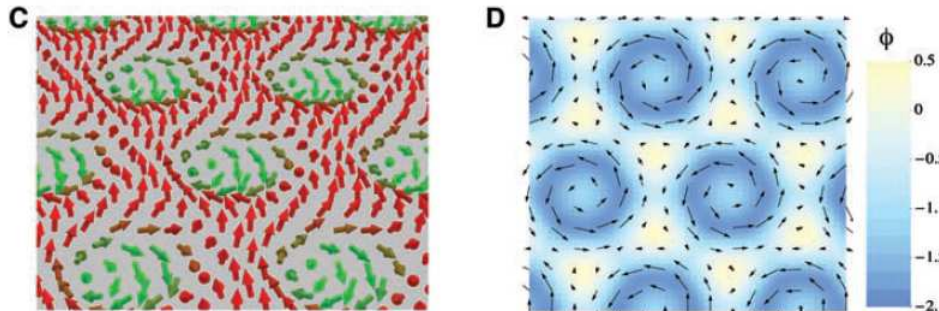


Magnetisation:

$$\mathbf{m} = m\mathbf{N}$$

Skyrmion Lattice in a Chiral Magnet

S. Mühlbauer,^{1,2} B. Binz,³ F. Jonietz,¹ C. Pfleiderer,^{1*} A. Rosch,³
A. Neubauer,¹ R. Georgii,^{1,2} P. Böni¹

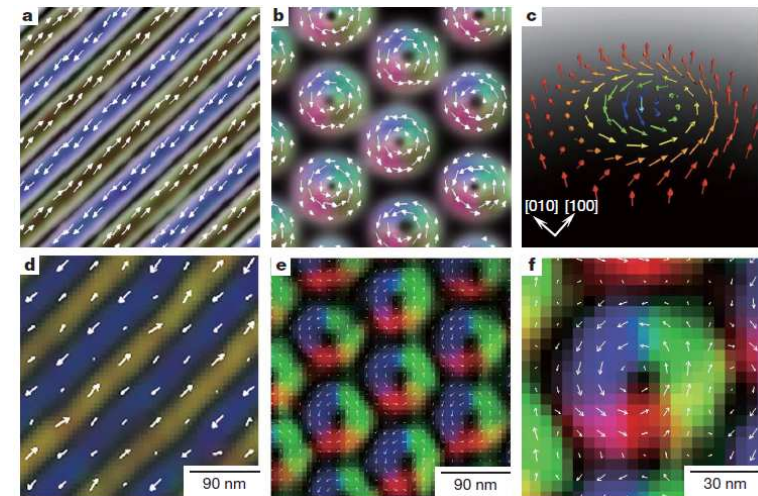


chiral itinerant-electron magnet **MnSi**

www.sciencemag.org **SCIENCE** VOL 323 13 FEBRUARY 2009

Real-space observation of a two-dimensional skyrmion crystal

X. Z. Yu^{1,2}, Y. Onose^{2,3}, N. Kanazawa³, J. H. Park⁴, J. H. Han⁴, Y. Matsui¹, N. Nagaosa^{3,5} & Y. Tokura^{2,3,5}



Topological spin textures in the helical magnet **Fe_{0.5}Co_{0.5}Si**.

NATURE | Vol 465 | 17 June 2010

Analogy liquid crystals and chiral ferromagnets

2/3

Free energy of chiral ferromagnets:

$$\mathbf{m} = m\mathbf{N}$$

$$f^M = Am^2(\nabla\mathbf{N})^2 + A\eta(\nabla m)^2 + rm^2 + bm^4 + Dm^2\mathbf{N} \cdot (\nabla \times \mathbf{N})$$

Free energy of chiral nematic liquid crystal:

$$Q_{ij} = S(3n_i n_j - \delta_{ij})/2$$

$$F = \int_{LC} \left[\frac{A_0(1-\gamma/3)}{2} Q_{ij}Q_{ij} - \frac{A_0\gamma}{3} Q_{ij}Q_{jk}Q_{ki} + \frac{A_0\gamma}{4} (Q_{ij}Q_{ij})^2 \right] dV$$

$$+ \frac{L}{2} \int_{LC} \left[\left(\epsilon_{ikl} \frac{\partial Q_{lj}}{\partial x_k} + 2q_0 Q_{ij} \right)^2 + \left(\frac{\partial Q_{ij}}{\partial x_i} \right)^2 \right] dV$$



$$f^{LC} = \frac{9}{4}LS^2(\nabla\mathbf{n})^2 + \frac{3}{4}L(\nabla S)^2 + \frac{3}{4}aS^2 + \frac{1}{4}cS^3 + \frac{9}{16}dS^4 + \frac{9}{2}q_0LS^2\mathbf{n} \cdot (\nabla \times \mathbf{n})$$

Mapping of parameters: $A \leftrightarrow 9L/4$, $\eta \leftrightarrow 1/3$, $r \leftrightarrow 3a/4$, $0 \leftrightarrow c/4$, $b \leftrightarrow 9c/16$

IMPORTANT: magnetisation \mathbf{m} is vector field, whereas LC director \mathbf{n} is vector with \mathbf{n} to $-\mathbf{n}$ symmetry

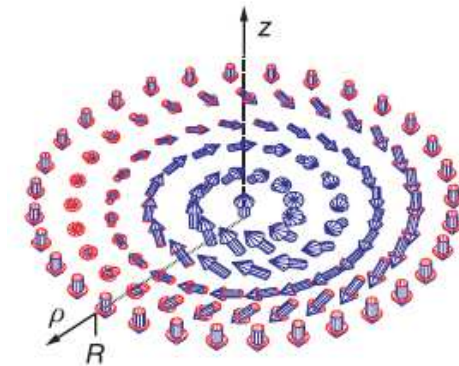
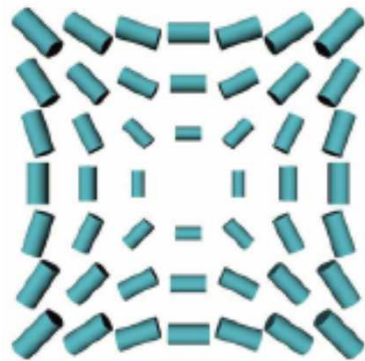
Analogy liquid crystals and chiral ferromagnets

3/3

Nematic escaped singular loops – bubble gum defects

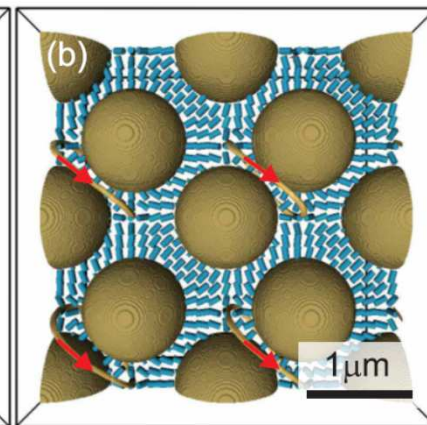
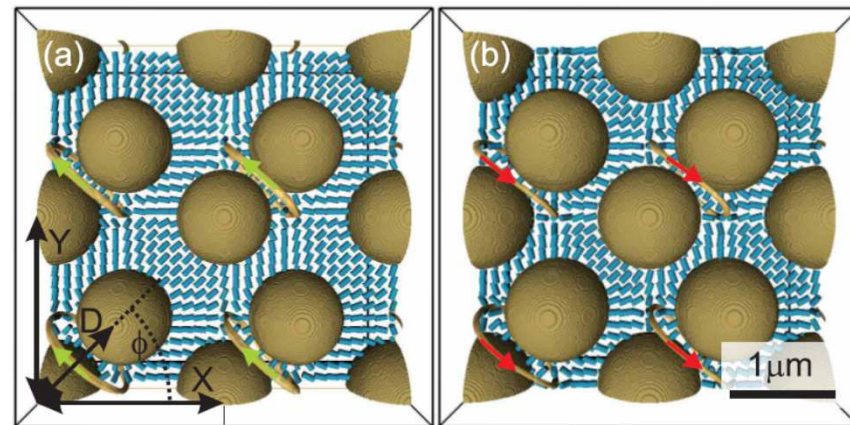
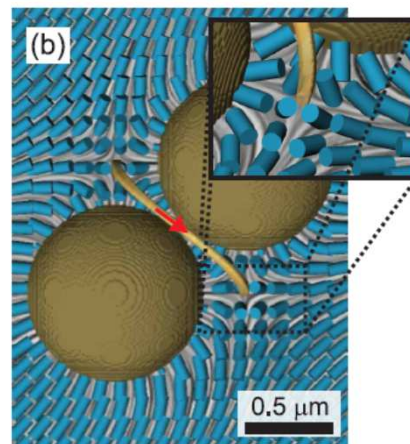
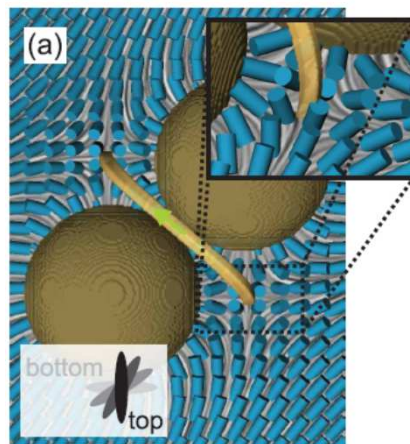
PRL 09

Hyperbolic -1 defect line

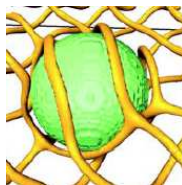
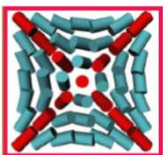
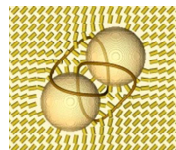
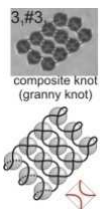
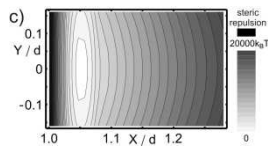
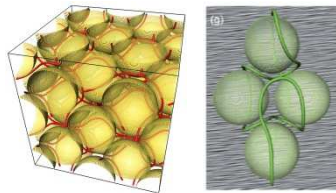
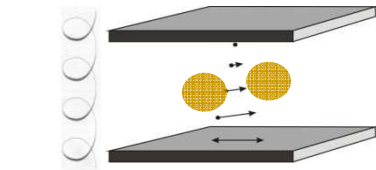


Escape into the 3rd dimension

Particle dimers and 2D crystals: loops of escaped -1 defect lines



Conclusions



- Temperature quench is an efficient mechanism for generation of topological defect loops
- Nematic colloids can stabilise various defect loop conformations; within 1D, 2D and 3D particle structures
- Typical free energy differences between (meta)stable structures are $\sim 1\%$; yet corresponding to $\sim 1000kT$.
- Energy barriers between states are strongly anisotropic and much higher than $100-1000kT$.
- Twisted “environment” gives energetic stabilisation of structures with further complexity:

assembly of arbitrary knots and links

Two possibly interesting systems that could give complex topology: liquid crystal blue phases, skyrmion structures.